13th World Conference on Earthquake Engineering
Vancouver, B.C., Canada
August 1-6, 2004
Paper No. 3153

RELEVANCE OF R-FACTOR AND FUNDAMENTAL PERIOD FOR SEISMIC DESIGN OF TUNNEL FORM BUILDINGS

Can BALKAYA[1] and Erol KALKAN[2]

SUMMARY

In many seismic design codes and guidelines, such as UBC (1997), NEHRP provisions (ASCE 2000) and Turkish Seismic Code (1998), reduction in seismic forces via response modification factor (R) is justified by the unquantified overstrength and ductile response of buildings during design earthquake. However, none of these references address R-factor for RC buildings composed of solely shear walls without accommodating any columns and beams. The typical implementation of such a structural system is reflected in multi-storey reinforced concrete tunnel form buildings. The unique lateral and vertical load transferring mechanism and ease of construction of tunnel form buildings lead them as the prevailing structural type especially in the regions prone to high seismic risk. This paper first addresses the evaluation of a consistent R-factor for their seismic design. Inelastic static pushover analysis was utilized for that purpose on a three-dimensional (3D) highly detailed model. Second, consistency of code-based empirical equations to explicitly estimate the fundamental period of tunnel form buildings was evaluated. The results of analyses show that conventional empirical equations are incapable of predicting the true fundamental period of tunnel form buildings. Based on the premise that such simplified equations are commonly used in practice, a new predictive equation was proposed herein. This equation was developed based on the 3D analyses of 140 tunnel form buildings having a variety of plans, heights and shear-wall configurations. Comparisons with experimental results show good correlation, and lend further credibility to proposed equation for its use in practice.

INTRODUCTION

Multi-storey reinforced concrete (RC) tunnel form buildings (i.e., box type buildings) are finding widespread use in seismic regions. The main ingredients of such buildings are their relatively thinner shear-walls and flat-slabs compared to those of traditional RC buildings. Shear-walls in tunnel form buildings are utilized as the primary lateral load resisting and vertical load carrying members due to absence of beams and columns. The typical implementation of a tunnel form system and its details are exhibited in Figure 1.

[1] Assoc. Prof., Middle East Technical University, Turkey. Email: cbalkaya@metu.edu.tr
[2] PhD. Student, University of California Davis, CA, USA. Email: ekalkan@ucdavis.edu

In a tunnel form system, load carrying pre-cast members are avoided, whereas non-structural pre-cast elements such as RC stairs and outside facade panels (Fig.1) are widely used to expedite the construction. Continuity of shear-walls throughout the height is recommended to avoid local stress concentrations and minimize torsion. Such a strict shear-wall configuration in the plan and throughout the height of the building may limit the interior space use from an architectural point of view, and it is one of the disadvantages of the tunnel form buildings. During construction, walls and slabs, having almost the same thickness, are cast in a single operation. That process reduces not only the number of cold-formed joints, but also the assembly time. The simultaneous casting of walls and slabs results in monolithic structures unlike any other frame type RC buildings. Consequently tunnel form buildings gain enhanced seismic performance by retarding plastic hinge formations at the most critical locations, such as slab-wall connections and around wall openings [4].

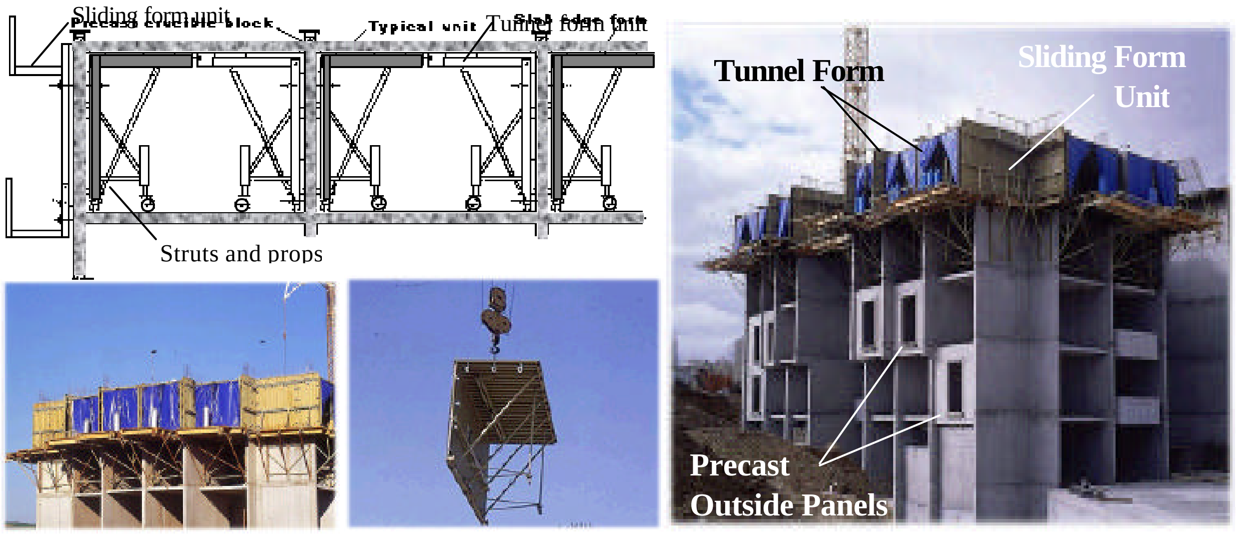

Figure 1. Tunnel form building construction system

Seismic performances of tunnel form buildings have recently been observed during the 1999 earthquakes (Mw 7.4 Kocaeli and Mw 7.2 Duzce) in Turkey. These earthquakes hit the most populated environments, and caused substantial structural damage, casualties and economic loss. In the aftermath of this misfortune, neither demolished nor damaged tunnel form buildings located in the vicinity of damage-suffering regions were reported in contrast to severely damaged conditions of many conventional frame-type RC buildings. Such performance of tunnel form buildings has stimulated their construction in Turkey in replacement of many severely damaged and collapsed RC buildings. Not only in Turkey, but also in many other countries prone to seismic risk, tunnel form buildings are gaining an increasing popularity. That accentuates an urgent need to clarify their seismic behavior, design and safety issues.

Therefore, this paper mainly focuses on evaluation of two important design parameters, response modification factor (*R*-factor) and fundamental period for the seismic design of tunnel form buildings. The development of a consistent R-factor based on inelastic static pushover analysis results of a typical tunnel form building is presented in the proceeding sections. Thereafter development of a simple empirical formula to estimate the fundamental period of tunnel form buildings is presented. This formula was developed based on the finite element analysis of 140 tunnel form buildings having a variety of plans, heights and shear-wall configurations.

MODEL DEVELOPMENT FOR INELASTIC STATIC ANALYSIS

By way of evaluating the 3D nonlinear seismic response of tunnel form buildings, 5-story residential building was modeled in finite element domain. The building details are given in Figure 2. The structural system is composed of solely shear-walls and slabs having the same thickness (12 cm) as usual applications. It is of interest to note that almost equal slab and wall thickness, generally less than that of used in conventional RC structures having analogous architectural plans, causes a high slab-wall interaction [5]. Therefore, for the modeling of such structures, making a rigid diaphragm (infinitely rigid in their own plane) assumption in order to simplify the analysis and save from the execution time does not necessarily reflect their realistic behavior. This may be attributed to fact that tunnel form buildings behave like thin-wall-tubular structures where in-plane rigidity is low [6]. Thus, high stress-concentrations may increase the crack propagation at the edges of slab-wall connections. To better reflect the in-plane floor flexibility and the slab-wall interaction, it is more reasonable to model the shear-walls and slabs by using finite elements having both flexural and membrane capabilities. Towards this aim, a new nonlinear shell element was developed using an isoparametric serendipity interpolation scheme with 5 d.o.f. per node [4]. This form of element description was selected in order to have a variable order of displacement definition possible along each of the element edges for representing more realistic reinforcement contribution.

To reduce the computational time as well as the capacity associated with the 3D modeling of incorporating shell elements, a mixture of finite elements of different order was used. Higher order finite elements were utilized at the critical locations where stress concentrations or stress gradients were expected to be high. In all models the shear-walls were modeled as sitting on the fixed base supports and soil effects were ignored. The reinforcements were modeled as discrete or embedded based on the criticality of their locations. The minimum amount of steel percentage taken in the analyses for shear-walls and slabs was 0.4 percent of the section area in accordance with the ACI 318 [7] specifications. There were also additional longitudinal and diagonal reinforcement used in the modeling in the form of 2 #4 (13 mm in diameter) at the inner and outer faces of the edges and 2#4 around the openings. During all analyses, geometric nonlinearity was disregarded due to the formation of the relatively small deformations, whereas only material nonlinearity was considered as necessary. The material properties of the concrete and the steel used in the analytical model are presented in Table 1.

Table 1. Material properties of concrete and steel

Concrete	Steel	Steel Rod Element
$E = 2.14\text{x}10^6$ t/m^2	$E = 2\text{x}10^7$ t/m^2	$E = 2\text{x}10^7$ t/m^2
$\nu = 0.2$	$\nu = 0.0$	$\nu = 0.3$
$f_{tu} / f_{cu} = 0.06823$	Q_s(top) = 0.2% in both directions	$A_s = 0.000226$ m^2 (at openings)
$f_{c28} = 1925$ t/m^2	Q_s(bot.) = 0.2% in both directions	$A_s = 0.000452$ m^2 (at edges)
	fy = 22000 t/m^2	fy = 22000 t/m^2

Nonlinear Isoparametric Shell Element

A nonlinear isoparametric shell element providing the capability of a variable edge order and arbitrarily placed movable edge nodes (to consider the location, and amount of main reinforcement near the edges and around the openings as discrete reinforcement) was developed and implemented to POLO-FINITE [8]. The rest of the analyses were performed by using this general purpose nonlinear finite element analysis program. The capability of moving any of the element's edge nodes to any location along an edge allows these edge nodes to be placed in the proper position that they can serve as end nodes for the cover of the main discrete reinforcement. That provides a robust stiffness contribution coming from the main reinforcement [9]. Besides arbitrarily movable edge nodes, the advantage of a variable edge order in the finite element modeling can be put to good use when the stress gradients are expected to be high. This allows increasing the order of the displacement field in critical areas such as around openings and slab-wall connections. The matching of the displacement fields between different order finite elements can be adjusted to retain the compatibility along their common edges. One of the improvements resulting from the use of this element is the reduction in the capacity and computational time required to reach a solution while retaining the level of accuracy deemed desirable. In this study, the shape of the stress-strain curve, tension stiffening and the cracking having opening and closing capability [10, 11] were considered in the context of the material nonlinearity.

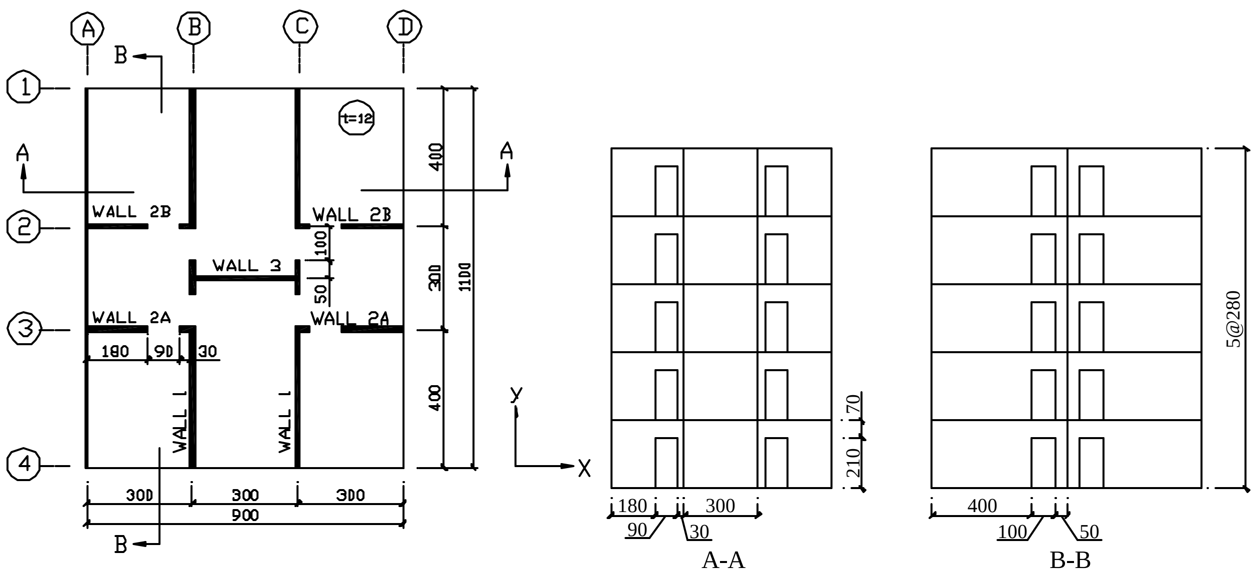

(a) Plan View

(b) Elevation

Figure 2. Details of 5-story building, units are in cm

Reinforcement Modeling

Finite element modeling of the reinforcement in a reinforced concrete member can be handled in a number of different ways. The steel can be considered as discrete steel elements, as individual steel units embedded in a concrete element, or as a smeared layer of steel sandwiched within the concrete layers. In the discrete model, reinforcing bars can be modeled using special rod elements located between prescribed element edge nodes. In general, these are two nodded elements that present compatibility discontinuities with the adjacent concrete units. Higher order elements can be used along the edges of comparable order concrete elements. If a higher order element is desired with the steel placed to pass through the interior of an element, an embedded steel element should be preferred. On the other hand, the smeared reinforcement model, that is the easiest to implement, transfers the effects of the steel directly into the concrete element. In this study, nonlinear rod elements were used around the openings, and discrete rebars having elasto-plastic stress-strain characteristics were preferred near the edges. With the help of the developed isoparametric shell element, the discrete steel could be included while locating the rebars with proper concrete cover requirements. With a two noded rod element, the stiffness contributed only to its end nodes. For this case, the bond was neglected due to the incompatible nature of the two displacement fields defining the deformations of the steel and concrete. In this study, the smeared steel model was used as the general reinforcement for non-critical locations. It was treated as an equivalent uniaxial layer of the material at the appropriate depth and smeared out over the element as several orthotropic layers. The steel is taken into account in both faces of the slabs and shear-walls, and in both principal directions considering the minimum steel ratio and cover thickness.

Crack Modeling

Cracks in concrete can be modeled either as a smeared or a discrete crack model. In the smeared crack modeling, there are several options. They can be modeled either as a fixed-crack or as a rotational-crack. In most of the finite element analysis of RC structures, crack directions are assumed to be fixed; this means when the crack forms it remains open. However, this model leads to crack directions that can be inconsistent with the limit state [12]. The change in the crack direction and the consequential change in the direction of the maximum stiffness were clearly observed in the experiments of Vecchio and Collins [13]. Therefore, the need for an algorithm that accounts this rotating crack effects is inevitable. In fact, the rotating crack models represent the actual behavior more accurately [10]. The constitutive matrix implemented in this study has been derived by Gallegos and Schnobrich [11]. The important concrete cracking behavior was handled through the smeared crack concept that has a rotation as well as closing and opening capabilities. More comprehensive information regarding the capabilities of the isoparametric shell element was given by Balkaya and Kalkan [4].

DEVELOPMENT OF CAPACITY DIAGRAM

In order to evaluate the capacity diagram [14] to be used later for computation of R-factor, inelastic static pushover analyses were performed on the 2D and 3D computer models of the 5-story building. 2D model was simulated considering only the main shear-walls (Section B-B in Fig. 2). During pushover analyses, gravity loads were applied to structures first, thereafter pushed with incrementally increased static equivalent earthquake loads (inverted triangle) up to the limits of the structure. Previous studies showed that [4,5,6,15] torsion is an important behavior appearing in the first vibration mode of tunnel form buildings due to the tunnel form construction restrictions. As such, part of the outside walls should be opened in order to take the formwork back during construction (Fig.1), that limitation reduces the torsional rigidity of the structure. The approach for considering the effects of torsion in the development of capacity diagram is described in ATC-40 [14]. This procedure was followed in this study due to the appearance of torsion in the first mode of the model structure. The resulting modified capacity curves for the 2D and 3D analysis of 5-story building as a result of the applied lateral loading in the y-direction (Fig. 2) are shown in Figure 4. These curves correspond to the last loading step of pushover analysis where excessive crack development at the base level of shear-walls did not yield any more plastic deformation. Comparing to 2D model, 3D model gives higher capacity level. The base moments and resultant forces were calculated considering couple walls to observe the contribution of the 3D behavior [6]. For 5-story building, global yielding occurred at the location of the shear-wall bases and the connection joints around the openings. A combination of a distributed shear-wall mechanism and a story mechanism lead to the collapse stage accompanying the inelastic deformation. The overall system behavior was completely controlled by the symmetrically distributed shear-walls. Further details of applied 3D pushover analyses and its implementation under dominant torsional effects were discussed in Balkaya and Kalkan [4].

The capacity spectrum is assumed to uniquely define the structural capacity irrespective of the earthquake ground motion input. However, in order to reach a comparable conclusion about the expected demand of structures under design earthquake levels, the obtained capacity curves should be plotted on the same format with the selected demand spectrum. This trend has been followed for performance evaluations in recent years. Herein the demand curve is represented by earthquake response spectra. In general, a 5 percent damped response spectrum is used to represent the demand when the structure is responding linearly elastic. The capacity curves were converted into the acceleration displacement response spectrum format (ADRS) for comparison with demand curves. This procedure required making adjustments on the capacity curve by the modal mass coefficient and the modal participation factor of the first natural mode of the building. The effective vibration periods of the 5-story building obtained from the modal analysis was 0.230 sec. The building was pushed to roughly 2.10 cm of roof displacement in 3D analysis. The structural behavior type was selected as *Type A* according to ATC-40. The obtained values of the modal participation factors (PF_{RF}) and the effective mass coefficients ($?_m$) were 1.38 and 0.76, respectively. The seismic demand was determined in accordance with the current Turkish Seismic Code [3]. The corresponding seismic demand and capacity spectra are presented in the ADRS format for comparison in Figure 4. The energy dissipation capacity of the 5-story building is corresponds to 24.6 percent equivalent viscous damping (a_y=0.31g, d_y=0.41cm, a_p=0.51g, d_p=1.52cm). The results show that the building was capable of satisfying the code requirements at the acceleration sensitive region of the design spectra. The capacity and demand intersect at a performance point where the roof displacement to the total height ratio is 0.0015. At this level, the building is considered to be satisfying the immediate occupancy (IO) performance level according to ATC-40.

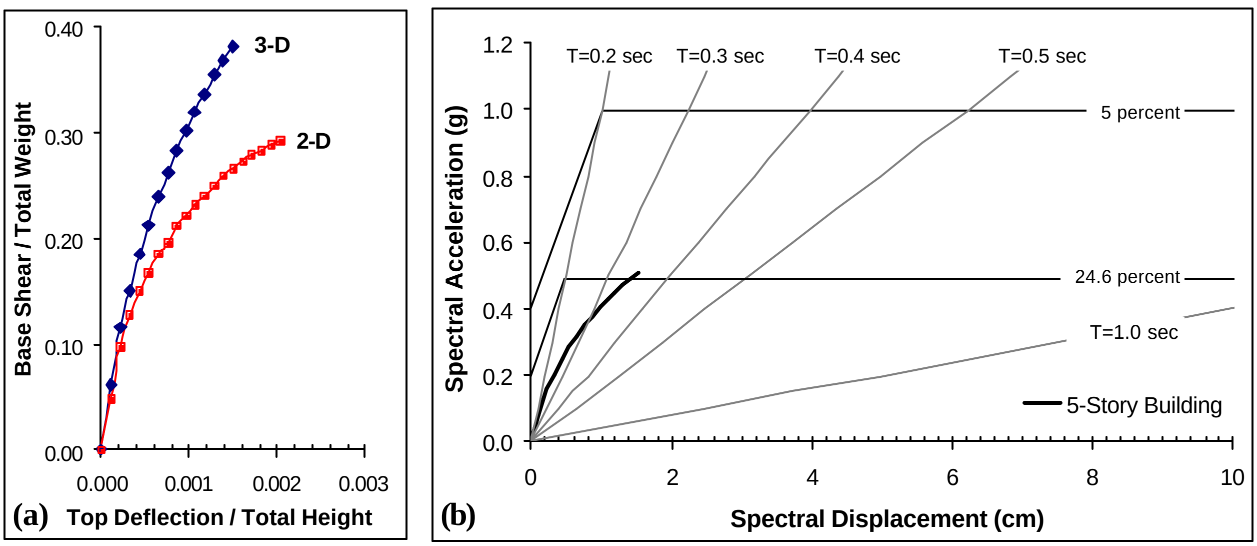

Figure 4. (a) Modified capacity curves for 3D and 2D models of 5-story building; (b) Performance evaluation according to ATC-40 considering the Turkish Seismic Code (1998) design spectrum (soft soil site condition)

RESPONSE MODIFICATION FACTOR, (R-FACTOR)

In many seismic design codes and guidelines, such as UBC [1], NEHRP provisions [2] and TSC [3], reduction in seismic forces via response modification factor (*R-Factor*) is justified by the unquantified overstrength and ductile response of buildings during design earthquake. However, none of these references address R-factor for RC buildings composed of solely shear-walls. In order to obtain a consistent R-factor for tunnel form buildings results of previously discussed inelastic static pushover analysis of the 5-story building is used herein.

The values assigned to R-factor are generally intended to account for the period-dependent ductility factor ($R_{??}$), period-dependent overstrength factor (R_S), and redundancy (R_R) factor. In this way R-factor can simply be expressed as their product [16]:

$$R = (R_S \, R_{??}) \, R_R \tag{1}$$

Recent developments in the displacement based design methodology [2, 14] enable more quantitative evaluation of these factors. The relations exhibited in Figure 5 can be established for that purpose. In this figure the redundancy factor was developed as part of the project ATC-34 [17]. That is proposed to quantify the improved reliability of seismic framing systems that use multiple lines of vertical seismic framing in each principal direction of a building [18]. For our studied case, this factor can be taken as one. For the evaluation of the other two factors, the seismic design parameters, such as seismic zone, site geology and fundamental period must be clearly identified as a priori. Accordingly, the worse scenario (highest seismicity and soft-soil site condition) based on the TSC [3] was chosen. That corresponds to a design base shear value of 0.25W for the 5-story building. The overstrength factor (R_S), which can be determined as the ratio of the maximum lateral strength of a building (V_u) to the yield strength (V_{fy}), envelopes the global effects of story drift limitations, multiple load combinations, strain hardening, participation of nonstructural elements, and other parameters [19]. This relation and its sources has been the subject of much research in recent years [20, 21, 22]. To quantify this value, Hwang and Shinozuka [23] studied a 4-story RC intermediate moment frame building located in seismic zone 2 as per the UBC, 1994 [24], and they reported an overstrength factor of 2.2. Mwafy and Elnashai [25] performed both inelastic static pushover and time-history collapse analyses on 12 RC frame type buildings designed based on the EC8 codes [26] and having various heights and lateral load supporting systems. They have declared that all studied buildings have overstrength factors over 2. For the investigated case here, the overstrength factor was calculated as 1.96. It is expected that their actual values may be higher than those estimated due to the contribution of nonstructural components.

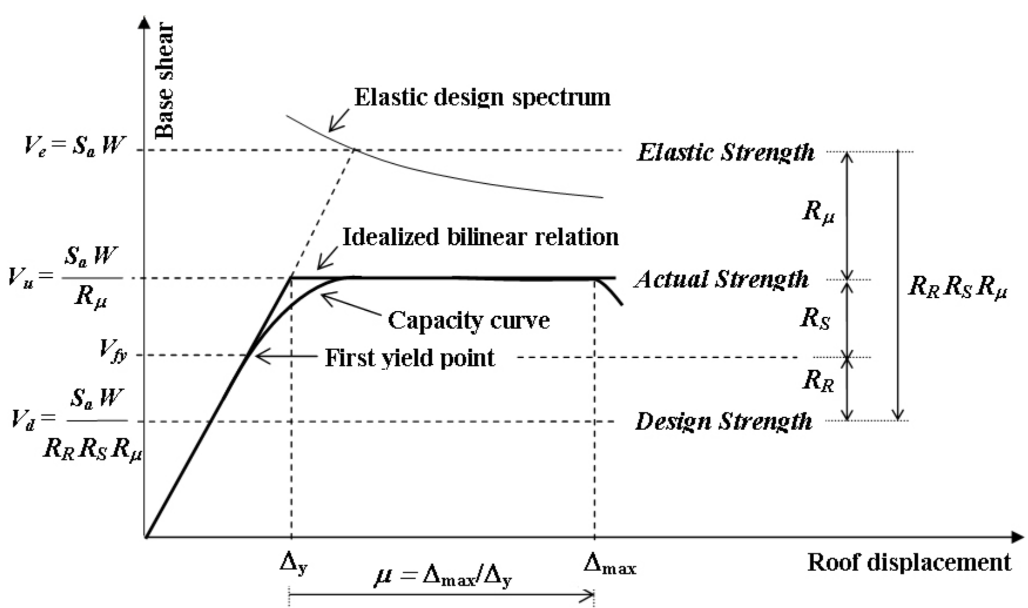

Figure 5. Relationships between the response modification factor (R), ductility factor ($R_{??}$) and overstrength factor (R_S)

The ductility factor (*R?*) is a measure of the global nonlinear response of the system [5]. Basically this parameter can be expressed as the ratio of elastic to inelastic strength (e.g. [25]) as illustrated in Figure 5. The resultant ductility factor was found as 2.0 for 5-story building. It may yield to response modification factor of 4.0 according to Equation (1). The imposed *R*-factor in current seismic codes for RC frame type structures having shear-wall system that might be accepted as the closest form to tunnel form buildings is equal to 5.5 in the UBC1997 and 4.0 or 6.0 (depending on the ductility level) in the TSC [3]. This comparison shows that values given in these references are admissible for the 5-story building investigated. It is certain that standardization of a response modification factor entails further investigations on a numerous tunnel form buildings having different plan and height combinations.

A SIMPLE FORMULA FOR FUNDAMENTAL PERIOD ESTIMATION

It is customary in practice to obtain the lower bound fundamental period of a structure via code-given expressions to establish the proper design force level unless modal analysis based on the detailed finite element model is conducted. Therefore accurate estimation of the fundamental period is inevitably essential to calculate the reliable design forces. It has long been realized that significant errors are tend to occur when the code-given equations such as those given in the UBC1997 [1] and TSC [3] are utilized for shear-wall dominant systems [15, 27]. To compensate for this deficiency, Lee et al. [27] proposed a simple formula based on their experimental data to estimate the lower bound fundamental period of tunnel form buildings having stories = 15. A set of new formulas to estimate the period of such buildings having stories = 15 has recently been developed by Balkaya and Kalkan [15]. The objective here is to present updated information on the period of such buildings using an extended building inventory as the continuation of our earlier work. Therefore, a simpler formula that can be applicable for both mid-rise (storey level =15) and high-rise (storey level >15) tunnel form buildings is developed based on the finite element analyses of 20 different buildings (most have as-built plans and are already constructed). Each building was studied for 7 different storey levels (i.e., 5, 10, 12, 15, 18, 20 and 25). Shear-wall thickness was taken as 12 cm for buildings up to 15 stories, 15 cm for 18-story buildings and 20 cm for 20- and 25-story buildings. The database compiled constitutes 140 buildings, their plan dimensions, number of stories and heights, shear-wall areas in two plan directions as well as computed fundamental periods using 3D FEM analyses. This ensemble is presented in Table 2. The equation developed to predict the fundamental period of the tunnel form buildings has the following form

$$T ? Ch\frac{\sqrt{R}}{(R^{a}_{length} ? R^{a}_{width})} \tag{2}$$

where T is the period in sec, h is the total height of building in m; R *is the r*atio of long side dimension to short side dimension of the building; R_{length} is the ratio of shear-wall area oriented along the length to typical story area; and R_{width} is the ratio of shear-wall area oriented along the width to typical story area. In this equation C and a are the estimator parameters obtained from regression analysis, and are equal to 0.138 and -0.4, respectively. The results obtained were also used to compute the associated errors in the estimation. The standard deviation of residuals, $?_T$, expressing the random variability of periods, is 0.3 and the value of R^2 (i.e., indication of goodness of fit) is equal to 0.80. There is no significant bias observed from the investigation of residuals. Equation (2) is similar to code equations (e.g. [1], [3]) except for the three new parameters that we introduced. Analysis of results herein and from our earlier studies show that tunnel form buildings are significantly susceptible to torsion due to the plan shear-wall configuration that is restricted by the tunnel form construction technique (first mode deformed shapes of the buildings are also described in Table 2). To account for this behavior and the effects of shear-walls into the period estimation, an additional parameter, R, is plugged into Equation (2) incorporating two other parameters, R_{width} and R_{length}.

Table 2. Structural and dynamic properties of buildings

Plan	# of	Height	Dimension (m)		Shear wall Area (m^2)		FEM Results		Predicted Period T(sec)		
No	Story	(m)	Length	Width	Length	Width	T (sec)	1st Mode	Equation (1)	TSC98	UBC97
1	5	14.0	29.70	15.70	4.78	17.80	0.13	Long.	0.27	0.17	0.17
	10	28.0	29.70	15.70	4.78	17.80	0.29		0.53	0.38	0.37
	12	33.6	29.70	15.70	4.78	17.80	0.37		0.64	0.45	0.44
	15	42.0	29.70	15.70	4.78	17.80	0.49		0.80	0.55	0.54
	18	50.4	29.70	15.70	5.98	22.25	0.70		1.05	0.57	0.57
	20	56.0	29.70	15.70	7.97	29.67	0.74		1.31	0.54	0.54
	25	70.0	29.70	15.70	7.97	29.67	1.03		1.64	0.65	0.64
2	5	14.0	31.04	19.92	3.40	19.92	0.12	Long.	0.20	0.15	0.15
	10	28.0	31.04	19.92	3.40	19.92	0.28		0.40	0.35	0.35
	12	33.6	31.04	19.92	3.40	19.92	0.35		0.48	0.42	0.42
	15	42.0	31.04	19.92	3.40	19.92	0.47		0.60	0.52	0.52
	18	50.4	31.04	19.92	4.25	24.90	0.58		0.79	0.55	0.54
	20	56.0	31.04	19.92	5.67	33.20	0.64		0.99	0.52	0.52
	25	70.0	31.04	19.92	5.67	33.20	0.95		1.24	0.63	0.62
3	5	14.0	38.80	17.03	3.98	19.60	0.14	Long.	0.25	0.18	0.18
	10	28.0	38.80	17.03	3.98	19.60	0.31		0.49	0.39	0.39
	12	33.6	38.80	17.03	3.98	19.60	0.39		0.59	0.47	0.46
	15	42.0	38.80	17.03	3.98	19.60	0.50		0.74	0.57	0.57
	18	50.4	38.80	17.03	4.98	24.50	0.59		0.97	0.60	0.59
	20	56.0	38.80	17.03	6.64	32.67	0.64		1.21	0.57	0.56
	25	70.0	38.80	17.03	6.64	32.67	0.93		1.51	0.68	0.67
4	5	14.0	12.00	8.00	1.44	2.88	0.14	Trans.	0.25	0.32	0.32
	10	28.0	12.00	8.00	1.44	2.88	0.35		0.50	0.61	0.77
	12	33.6	12.00	8.00	1.44	2.88	0.49		0.60	0.70	0.94
	15	42.0	12.00	8.00	1.44	2.88	0.76		0.75	0.82	1.18
	18	50.4	12.00	8.00	1.80	3.60	1.01		0.99	0.95	1.25
	20	56.0	12.00	8.00	2.40	4.80	1.17		1.23	1.02	1.18
	25	70.0	12.00	8.00	2.40	4.80	1.81		1.54	1.21	1.43
5	5	14.0	12.00	8.00	3.84	1.92	0.16	Torsion	0.28	0.36	0.42
	10	28.0	12.00	8.00	3.84	1.92	0.43		0.56	0.61	0.80
	12	33.6	12.00	8.00	3.84	1.92	0.55		0.68	0.70	0.93
	15	42.0	12.00	8.00	3.84	1.92	0.74		0.84	0.82	1.12
	18	50.4	12.00	8.00	4.80	2.40	0.89		1.11	0.95	1.15
	20	56.0	12.00	8.00	6.40	3.20	0.97		1.38	1.02	1.08
	25	70.0	12.00	8.00	6.40	3.20	1.28		1.73	1.21	1.29
6	5	14.0	12.00	8.00	1.44	3.84	0.11	Long.	0.26	0.30	0.29
	10	28.0	12.00	8.00	1.44	3.84	0.32		0.53	0.61	0.71
	12	33.6	12.00	8.00	1.44	3.84	0.45		0.63	0.70	0.86
	15	42.0	12.00	8.00	1.44	3.84	0.69		0.79	0.82	1.07
	18	50.4	12.00	8.00	1.80	4.80	0.93		1.04	0.95	1.13
	20	56.0	12.00	8.00	2.40	6.40	1.08		1.29	1.02	1.08
	25	70.0	12.00	8.00	2.40	6.40	1.68		1.61	1.21	1.30
7	5	14.0	12.00	8.00	2.88	2.64	0.13	Torsion	0.29	0.36	0.46
	10	28.0	12.00	8.00	2.88	2.64	0.35		0.57	0.61	0.84
	12	33.6	12.00	8.00	2.88	2.64	0.50		0.69	0.70	0.97
	15	42.0	12.00	8.00	2.88	2.64	0.75		0.86	0.82	1.15
	18	50.4	12.00	8.00	3.60	3.30	1.02		1.13	0.95	1.19
	20	56.0	12.00	8.00	4.80	4.40	1.18		1.40	1.02	1.11
	25	70.0	12.00	8.00	4.80	4.40	1.83		1.75	1.21	1.32
8	5	14.0	38.80	17.03	3.98	19.60	0.14	Torsion	0.25	0.36	0.44
	10	28.0	38.80	17.03	3.98	19.60	0.44		0.49	0.61	0.81
	12	33.6	38.80	17.03	3.98	19.60	0.58		0.59	0.70	0.94
	15	42.0	38.80	17.03	3.98	19.60	0.82		0.74	0.82	1.12
	18	50.4	38.80	17.03	4.98	24.50	1.03		0.97	0.95	1.16
	20	56.0	38.80	17.03	6.64	32.67	1.15		1.21	1.02	1.09
	25	70.0	38.80	17.03	6.64	32.67	1.69		1.51	1.21	1.29
9	5	14.0	12.00	8.00	4.80	1.92	0.16	Torsion	0.29	0.36	0.40
	10	28.0	12.00	8.00	4.80	1.92	0.43		0.58	0.61	0.75
	12	33.6	12.00	8.00	4.80	1.92	0.55		0.70	0.70	0.87
	15	42.0	12.00	8.00	4.80	1.92	0.74		0.88	0.82	1.04
	18	50.4	12.00	8.00	6.00	2.40	0.89		1.15	0.95	1.07
	20	56.0	12.00	8.00	8.00	3.20	0.98		1.43	1.01	1.01
	25	70.0	12.00	8.00	8.00	3.20	1.28		1.79	1.20	1.19
10	5	14.0	35.00	20.00	7.20	12.96	0.16	Long.	0.23	0.17	0.17
	10	28.0	35.00	20.00	7.20	12.96	0.38		0.46	0.39	0.39
	12	33.6	35.00	20.00	7.20	12.96	0.48		0.55	0.47	0.46
	15	42.0	35.00	20.00	7.20	12.96	0.64		0.69	0.57	0.57
	18	50.4	35.00	20.00	9.00	16.20	0.80		0.90	0.60	0.59
	20	56.0	35.00	20.00	12.00	21.60	0.92		1.12	0.57	0.56
	25	70.0	35.00	20.00	12.00	21.60	1.22		1.40	0.68	0.67

Table 2. Cont'd.

Plan No	# of Story	Height (m)	Dimension (m) Length	Dimension (m) Width	Shear wall Area (m^2) Length	Shear wall Area (m^2) Width	FEM Results T (sec)	FEM Results 1^{st} Mode	Predicted Period T(sec) Equation (1)	Predicted Period T(sec) TSC98	Predicted Period T(sec) UBC97
11	5	14.0	11.00	9.00	2.64	1.80	0.23	Torsion	0.23	0.34	0.33
	10	28.0	11.00	9.00	2.64	1.80	0.63		0.46	0.61	0.79
	12	33.6	11.00	9.00	2.64	1.80	0.82		0.56	0.70	0.95
	15	42.0	11.00	9.00	2.64	1.80	0.83		0.69	0.82	1.18
	18	50.4	11.00	9.00	3.30	2.25	1.35		0.91	0.95	1.24
	20	56.0	11.00	9.00	4.40	3.00	1.44		1.14	1.02	1.18
	25	70.0	11.00	9.00	4.40	3.00	1.94		1.42	1.21	1.42
12	5	14.0	31.50	27.15	9.70	13.86	0.16	Torsion	0.19	0.26	0.26
	10	28.0	31.50	27.15	9.70	13.86	0.42		0.37	0.61	0.63
	12	33.6	31.50	27.15	9.70	13.86	0.55		0.45	0.70	0.76
	15	42.0	31.50	27.15	9.70	13.86	0.77		0.56	0.82	0.95
	18	50.4	31.50	27.15	12.13	17.33	0.98		0.73	0.95	1.00
	20	56.0	31.50	27.15	16.17	23.10	1.10		0.91	0.96	0.95
	25	70.0	31.50	27.15	16.17	23.10	1.54		1.14	1.16	1.15
13	5	14.0	25.50	25.04	10.70	10.88	0.14	Torsion	0.19	0.19	0.19
	10	28.0	25.50	25.04	10.70	10.88	0.40		0.38	0.41	0.41
	12	33.6	25.50	25.04	10.70	10.88	0.55		0.46	0.49	0.48
	15	42.0	25.50	25.04	10.70	10.88	0.80		0.57	0.59	0.59
	18	50.4	25.50	25.04	13.38	13.60	1.03		0.75	0.62	0.61
	20	56.0	25.50	25.04	17.83	18.13	1.17		0.94	0.59	0.58
	25	70.0	25.50	25.04	17.83	18.13	1.69		1.17	0.70	0.69
14	5	14.0	28.00	12.00	2.88	3.60	0.13	Long.	0.23	0.30	0.29
	10	28.0	28.00	12.00	2.88	3.60	0.40		0.46	0.57	0.56
	12	33.6	28.00	12.00	2.88	3.60	0.54		0.55	0.66	0.65
	15	42.0	28.00	12.00	2.88	3.60	0.79		0.69	0.79	0.78
	18	50.4	28.00	12.00	3.60	4.50	1.02		0.90	0.81	0.81
	20	56.0	28.00	12.00	4.80	6.00	1.16		1.13	0.77	0.76
	25	70.0	28.00	12.00	4.80	6.00	1.70		1.41	0.91	0.90
15	5	14.0	27.00	24.00	8.40	13.55	0.17	Torsion	0.20	0.19	0.18
	10	28.0	27.00	24.00	8.40	13.55	0.49		0.39	0.40	0.39
	12	33.6	27.00	24.00	8.40	13.55	0.65		0.47	0.47	0.47
	15	42.0	27.00	24.00	8.40	13.55	0.92		0.59	0.57	0.57
	18	50.4	27.00	24.00	10.50	16.94	1.16		0.78	0.60	0.59
	20	56.0	27.00	24.00	14.00	22.58	1.32		0.97	0.57	0.56
	25	70.0	27.00	24.00	14.00	22.58	1.84		1.21	0.68	0.67
16	5	14.0	32.00	26.00	9.40	15.00	0.17	Torsion	0.19	0.17	0.17
	10	28.0	32.00	26.00	9.40	15.00	0.49		0.39	0.36	0.36
	12	33.6	32.00	26.00	9.40	15.00	0.64		0.47	0.43	0.43
	15	42.0	32.00	26.00	9.40	15.00	0.88		0.58	0.53	0.52
	18	50.4	32.00	26.00	11.75	18.75	1.10		0.77	0.55	0.55
	20	56.0	32.00	26.00	15.67	25.00	1.24		0.96	0.52	0.51
	25	70.0	32.00	26.00	15.67	25.00	1.69		1.20	0.62	0.62
17	5	14.0	24.00	14.00	4.80	7.44	0.17	Torsion	0.25	0.28	0.28
	10	28.0	24.00	14.00	4.80	7.44	0.48		0.50	0.55	0.54
	12	33.6	24.00	14.00	4.80	7.44	0.63		0.60	0.64	0.63
	15	42.0	24.00	14.00	4.80	7.44	0.88		0.75	0.77	0.76
	18	50.4	24.00	14.00	6.00	9.30	1.12		0.99	0.79	0.79
	20	56.0	24.00	14.00	8.00	12.40	1.29		1.23	0.75	0.74
	25	70.0	24.00	14.00	8.00	12.40	1.80		1.54	0.89	0.88
18	5	14.0	16.00	12.00	3.84	8.16	0.11	Torsion	0.27	0.32	0.32
	10	28.0	16.00	12.00	3.84	8.16	0.26		0.54	0.60	0.60
	12	33.6	16.00	12.00	3.84	8.16	0.33		0.64	0.70	0.69
	15	42.0	16.00	12.00	3.84	8.16	0.45		0.80	0.82	0.83
	18	50.4	16.00	12.00	4.80	10.20	0.59		1.06	0.86	0.85
	20	56.0	16.00	12.00	6.40	13.60	0.68		1.32	0.81	0.80
	25	70.0	16.00	12.00	6.40	13.60	1.03		1.64	0.96	0.95
19	5	14.0	28.00	12.00	5.76	6.00	0.13	Torsion	0.29	0.30	0.29
	10	28.0	28.00	12.00	5.76	6.00	0.40		0.59	0.57	0.56
	12	33.6	28.00	12.00	5.76	6.00	0.54		0.70	0.66	0.65
	15	42.0	28.00	12.00	5.76	6.00	0.79		0.88	0.79	0.78
	18	50.4	28.00	12.00	7.20	7.50	1.02		1.15	0.81	0.81
	20	56.0	28.00	12.00	9.60	10.00	1.16		1.44	0.77	0.76
	25	70.0	28.00	12.00	9.60	10.00	1.70		1.79	0.91	0.90
20	5	14.0	16.00	12.00	3.84	5.76	0.12	Trans.	0.25	0.33	0.33
	10	28.0	16.00	12.00	3.84	5.76	0.31		0.50	0.61	0.62
	12	33.6	16.00	12.00	3.84	5.76	0.39		0.61	0.70	0.72
	15	42.0	16.00	12.00	3.84	5.76	0.52		0.76	0.82	0.87
	18	50.4	16.00	12.00	4.80	7.20	0.64		0.99	0.90	0.89
	20	56.0	16.00	12.00	6.40	9.60	0.73		1.24	0.85	0.84
	25	70.0	16.00	12.00	6.40	9.60	1.06		1.55	1.01	1.00

* Long. implies longitudinal direction; Trans. implies transverse direction

COMPARISON WITH CODE-GIVEN PERIOD EQUATIONS

Performance of Equation (1) is next compared with code equations given in both the TSC [3] and UBC1997 [1]. Turkish Seismic Code [3] concerning the constructions in seismic areas has recently been modified in 1998. In TSC, the equation for predicting fundamental period of structures was taken directly from the UBC [1] with small modifications. The general form of the equation given in these provisions is as follows (note that all equations are in SI unit system):

$$T = C_t\,(h_n)^{3/4}\ (?\ 0.05) \tag{3}$$

where T is the period in seconds; C_t = 0.0853 (0.08) for steel moment-resisting frames, C_t = 0.0731 (0.07) for reinforced concrete moment-resisting frames and eccentrically-braced frames and C_t = 0.0488 (0.05) for all other buildings. Alternatively, the value of C_t for structures where seismic loads are fully resisted by reinforced concrete structural walls, can be taken as $0.0743(0.075)/(A_c)^{1/2}$. The numbers within the parentheses show the corresponding values given in the TSC. The value of A_c shall be calculated from the following formula:

$$A_c = ?\ A_e\,[0.2 + (D_e / h_n)^2] \tag{4}$$

The value of D_e/h_n used in Equation (4) shall not exceed 0.9. The period estimation via Equation (2) and also UBC and TSC equations were compared for various buildings in the database (Table 2). Also given in this table are the finite element analysis results as benchmark solutions. Comparisons show that there exists significant deviation between the FEM results and those computed using code equations. For many cases, code equations give a period much longer than computed for low- and mid-rise (i.e., 5, 10 and 12 stories) buildings, whereas for high-rise buildings (i.e., stories =15) reverse is observed, and they underestimate the computed periods. In fact, estimated periods should be the same or less than the actual period of the structure, thus their estimation should be conservative. In general comparisons reveal that there is a good agreement between estimated periods via Equation (2) and FEM results. For some of the 5-story buildings in the database, our equation could not capture the computed periods, and estimations result in higher deviation and become non-conservative.

COMPARISON WITH EXPERIMENTAL DATA

The estimated periods using Equation (2) are next compared with experimental data of Lee et al. [27] where the results of ambient surveys on fifty high rise tunnel form buildings having 15 to 25 stories were reported. The tested buildings have a wall thickness of 20 cm. The details of these buildings are listed in Table 2 including their plan dimensions, heights and shear-wall areas. The estimated fundamental periods via Equation (2) are also given in this table for comparison. The experimental data has two periods, one along longitudinal direction and second along transverse direction. On the other hand Equation (2) is aimed to estimate the fundamental period (first mode) regardless of the direction, attempting to consider the shear-wall configuration along both longitudinal and transverse directions as well as the effects of possible torsion. Therefore it may only yield a single value assumed as the fundamental period. Based on this premise, the comparisons show that Equation (2) gives estimates close to periods along the longitudinal direction for the majority of the buildings, but for only a few cases underestimates transverse periods or overestimates longitudinal periods. These results imply that Equation (2) is generally conservative as expected from any code-given equations. In fact, the period of the structures elongate during inelastic response because of stiffness degradation. Hence Equation (2) can be used to estimate the lower bound fundamental period of tunnel form buildings having stories 5 to 25. In this study, the effects of non-structural elements (e.g. outside panel walls) as well as local-site effects on period estimation were ignored (i.e., fixed support conditions were assumed in all computer models) but have been the part of our ongoing research. It should be noted that the proposed equation in this paper is based on the general consensus of engineering applications. Pending the accumulation of additional new data from the experimental studies and analysis of different buildings, the derived equation here can be progressively modified and improved.

Table 3. Comparison of results based on Equation (2) with experimental periods of Lee et al. [27]

Plan No **	# of Story	Height (m)	Dimension (m) Length	Dimension (m) Width	Shear wall Area (m^2) Length	Shear wall Area (m^2) Width	Measured Period T (sec) Long. *	Measured Period T (sec) Trans. *	Predicted Period T(sec) Equation (1)
1	15	40.0	38.98	11.26	13.17	24.58	1.92	0.71	1.42
2	15	40.0	27.22	12.83	10.48	18.16	N/A *	1.08	1.10
3	20	53.5	30.94	12.38	9.96	17.62	1.89	1.19	1.51
4	20	53.5	31.66	12.02	10.66	15.98	1.90	1.44	1.55
5	20	53.5	30.94	10.88	9.43	18.18	1.93	N/A	1.68
6	15	40.0	49.22	11.61	8.00	22.86	N/A	1.27	1.24
7	15	40.0	27.22	12.83	8.38	18.16	2.22	N/A	1.04
8	15	40.0	56.28	12.47	18.25	35.09	1.86	1.16	1.54
9	15	40.0	28.14	12.47	9.12	18.95	1.66	1.09	1.10
10	15	40.0	34.46	12.47	11.17	22.35	1.93	N/A	1.21
11	20	53.5	42.20	12.14	13.32	24.59	2.11	N/A	1.79
12	15	40.0	38.98	11.28	13.19	21.98	1.63	N/A	1.39
13	15	40.0	27.22	12.83	8.38	19.56	2.05	0.91	1.06
14	20	53.5	41.80	11.18	14.95	21.50	1.82	1.16	1.93
15	20	53.5	37.20	12.36	14.71	19.31	1.95	N/A	1.70
16	20	53.5	45.40	11.94	17.35	22.77	1.88	N/A	1.92
17	20	53.5	45.40	11.94	18.43	22.77	1.82	1.50	1.94
18	20	53.5	32.00	11.94	12.99	16.81	1.76	N/A	1.64
19	15	40.0	51.90	10.36	16.13	31.19	1.91	0.90	1.72
20	15	40.0	34.60	10.36	10.75	21.51	N/A	0.86	1.41
21	15	40.0	61.80	11.80	21.88	36.46	1.89	1.28	1.71
22	15	40.0	41.60	11.80	13.74	25.53	N/A	0.99	1.39
23	15	40.0	53.40	10.80	14.99	32.30	N/A	1.16	1.64
24	15	40.0	36.60	11.90	13.07	23.52	1.92	1.27	1.33
25	15	40.0	35.60	10.80	13.07	22.30	1.79	N/A	1.43
26	15	40.0	42.90	11.00	16.04	22.65	1.65	N/A	1.51
27	18	48.1	43.40	11.62	11.09	24.21	1.81	N/A	1.61
28	20	53.5	34.64	10.73	11.89	20.81	1.85	1.17	1.86
29	18	48.1	34.60	12.50	12.98	19.90	1.88	1.23	1.47
30	20	53.0	53.60	11.40	17.11	23.22	1.88	1.12	2.01
31	20	53.5	29.44	11.40	9.40	13.42	1.83	N/A	1.52
32	20	53.5	35.48	11.40	12.13	16.18	1.91	1.31	1.69
33	20	53.5	52.50	10.92	18.35	32.10	1.79	1.06	2.27
34	22	58.9	52.50	10.92	18.35	33.25	1.89	1.04	2.52
35	25	67.0	43.40	12.12	12.62	24.20	2.33	1.79	2.22
36	25	67.0	35.00	10.92	11.47	22.93	N/A	1.33	2.32
37	25	67.9	38.10	12.30	11.25	22.49	2.56	1.39	2.11
38	25	67.9	20.80	11.50	7.65	13.40	2.04	1.59	1.77
39	25	67.9	27.30	12.00	7.21	16.38	2.17	1.61	1.79
40	25	68.0	63.90	11.50	14.70	33.80	2.50	N/A	2.69
41	25	68.0	51.84	12.60	16.98	27.43	2.13	1.69	2.42
42	19	51.1	36.80	11.20	13.19	23.08	1.89	N/A	1.79
43	20	53.9	36.80	11.20	13.19	21.43	1.79	1.25	1.87
44	15	40.0	18.30	10.70	4.31	11.75	1.69	0.90	0.94
45	20	55.6	35.60	11.40	15.42	13.80	1.79	N/A	1.79
46	20	55.6	53.40	11.40	19.48	20.70	1.72	1.25	2.12
47	20	55.6	41.60	12.00	13.98	24.96	1.82	1.27	1.91
48	20	54.0	31.80	10.00	8.27	17.81	N/A	1.25	1.78
49	20	54.0	51.20	11.60	13.07	26.13	1.96	1.39	1.93
50	20	54.0	50.40	12.30	11.16	33.48	2.13	1.20	1.84

* Long. implies longitudional direction; Trans. implies transverse direction; N/A stands for not available

CONCLUSIONS

In this study, consistency of code-based empirical formulas to estimate the fundamental period of buildings was evaluated for tunnel form buildings. The comparative analysis results revealed that common formulas involved in the Turkish Seismic Code [3], and the Uniform Building Code [1] may yield inaccurate results for explicit determination of their fundamental period. Based on the premise that such formulas are commonly used in engineering practice, a new predictive equation was proposed herein. This equation was developed based on the finite element analysis of 140 buildings having a variety of plans, heights and wall-configurations. Comparisons with experimental results show good correlation, and lend further credibility to proposed equation for its use in practice.

The seismic performance evaluation of tunnel form buildings is performed based on the inelastic static analyses of a representative model. To accomplish a detailed 3D analysis a nonlinear isoparametric shell element having opening-closing and rotating crack capabilities was utilized. Thus more realistic behavior of shear-wall system was obtained. This efficiency facilitated the investigation of a consistent response modification factor for tunnel form buildings for their seismic design. The results of the presented study are considered to be an essential step regarding the reliable design and analysis of the buildings of concern against earthquake forces.

REFERENCES

1. UBC, Uniform Building Code (1997). International Conference of Building Officials. CA.
2. FEMA-356, (2000), Prestandard and commentary for the seismic rehabilitation of buildings, American Society of Civil Engineers (ASCE), Reston, VA.
3. Ministry of Public Works and Settlement (1998). 'Specifications for structures to be built in disaster areas', Ankara, Turkey.
4. Balkaya, C. and Kalkan, E. (2003). 'Nonlinear seismic response evaluation of tunnel form building structures', *Computers & Structures*. **81**, 153-165.
5. Balkaya, C. and Kalkan,, E. (2004). 'Seismic vulnerability, behavior and design of tunnel form buildings', *Engineering Structures*, (in review).
6. Balkaya, C. and Kalkan, E. (2004). 'Three-dimensional effects on openings of laterally loaded pierced shear-walls', *Journal of Structural Engineering, ASCE*. (in-press)
7. ACI 318 (1995). 'Building code requirements for reinforced concrete and commentary', ACI, Detroit, Michigan, 73-74, 218, 242.
8. POLO-FINITE, Structural mechanics system for linear and nonlinear, static and dynamic analysis. Dept. of Civil Eng., UIUC.
9. Balkaya, C. and Schnobrich, W.C. (1993). 'Nonlinear 3D behavior of shear-wall dominant RC building structures', *Struct. Eng. and Mech*. 1 (1), 1-16.
10. Milford, R.V. and Schnobrich, W.C. (1985). 'The application of the rotating crack model to the analysis of reinforced concrete shells', *Computers & Structures*. **20**, 225-234.
11. Gallegos-Cezares, S. and Schnobrich, W.C. (1988). 'Effects of creep and shrinkage on the behavior of reinforced concrete gable roof hyperbolic-paraboloids', *Struct. Research Series*. 543, UIUC.

12. Gupta, A.K. and Akbar, H. (1984). ‘Cracking in reinforced concrete analysis’, *Journal of Structural Engineering, ASCE*. 110 (8), 1735-1746.

13. Vecchio, F.J. and Collins, M.P. (1986). ‘The modified compression-field theory for reinforced concrete elements subjected to shear’, *ACI. Struct. J. Proc*. **83(**2), 219-231.

14. ATC-40 (1996). ‘Seismic evaluation and retrofit of concrete buildings’, Applied Technology Council, Redwood, CA.

15. Balkaya, C. and Kalkan, E. (2003). ‘Estimation of fundamental periods of shear-wall dominant building structures’, *Earthquake Eng. and Struct. Dyn*. **32**(7), 985-998.

16. ATC-19 (1995). ‘Structural response modification factors’, Applied Technology Council, Redwood, CA

17. ATC-34 (1995). ‘A critical review of current approaches to earthquake resistant design’, Applied Technology Council, Redwood, CA.

18. Whittaker, A., Hart, G. and Rojahn, C. (1999). ‘Seismic response modification factors’, *Journal of Structural Engineering, ASCE*. 125 (4), 438-444.

19. Uang, C-M. (1994). ‘Establishing R (or R_w) and C_d factors for building seismic provisions’, *Earthquake Eng. and Struct. Dyn*. **23**, 507-521.

20. Mitchell, D. and Paulter, P. (1994). ‘Ductility and overstrength in seismic design of reinforced concrete structure’, *Canadian Journal of Civil Engineering*. 21, 1049-1060.

21. Humar, J.L. and Ragozar, M.A. (1996). ‘Concept of overstrength in seismic design’, *Proc. of the 11th WCEE*. IAEE, Acapulco, Mexico, Paper No: 639.

22. Park, R. (1996). ‘Explicit incorporation of element and structure overstrength in the design process’, *Proc, of the 11th WCEE*. IAEE, Acapulco, Mexico, Paper No: 2130.

23. Hwang, H. and Shinozuka, M. (1994). ‘Effect of large earthquakes on the design of buildings in eastern United States’, *Proc. of the 5th U.S. National Conf. on Earthquake Eng*. Earthquake Engineering Research Institute, Oakland, CA, 223-231.

24. UBC, Uniform Building Code (1994). International Conference of Building Officials. CA.

25. Elnashai, A.S. and Mwafy, A.M. (2002). ‘Overstrength and force reduction factors of multistory reinforced- concrete buildings’, *The Structural Design of Tall Buildings*. **11**, 329-351.

26. CEN (Comite European de Normalisation) (1994). ‘Design provisions for earthquake resistance of structures’, Part 1-1, 1-2 and 1-3. Eurocode 8, European pre-standard ENV 1998-1-1, 1-2 and 1-3. CEN, Bruxelles.

27. Lee, L., Chang, K., Chun, Y. (2000). ‘Experimental formula for the fundamental period of RC buildings with shear-wall dominant systems’, *The Structural Design of Tall Buildings*. **9**(4), 295-307.